Agglomeration effects on the buckling behaviour of embedded concrete columns reinforced with SiO$_2$ nano-particles

Mehdi Zamanian, Reza Kolahchi[*] and Mahmood Rabani Bidgoli

Department of Civil Engineering, Jasb Branch, Islamic Azad University, Jasb, Iran

Abstract. The use of nanotechnology materials and applications in the construction industry should be considered for enhancing material properties. However, the nonlinear buckling of an embedded straight concrete columns reinforced with silicon dioxide (SiO2) nanoparticles is investigated in the present study. The column is simulated mathematically with Euler-Bernoulli and Timoshenko beam models. Agglomeration effects and the characteristics of the equivalent composite are determined using Mori-Tanaka approach. The foundation around the column is simulated with spring and shear layer. The governing equations are derived using energy method and Hamilton's principal. Differential quadrature method (DQM) is used in order to obtain the buckling load of structure. The influences of volume percent of SiO2 nanoparticles, geometrical parameters and agglomeration on the buckling of column are investigated. Numerical results indicate that considering agglomeration effects leads to decrease in buckling load of structure.

Keywords: agglomeration; buckling; concrete column; SiO$_2$ nanoparticles; DQM

1. Introduction

Concrete can be nano-engineered by incorporating nano-sized building blocks or objects (e.g., nanoparticles and nanotubes) to control material behaviour and add novel properties, or by grafting molecules onto cement particles, cement phases, aggregates, and additives (including nano-sized additives) to provide surface functionality, which can be adjusted to promote specific interfacial interactions. The nanoparticle is the elementary building block in nanotechnology and is comprised of up to thousands of atoms combined into a cluster of 1-100 nm. Nanoparticles have been shown to significantly enhance the mechanical performance of a variety of materials, including metals, polymers, ceramic, and concrete composites (Sobolev and Ferrada-Gutiérrez 2005, Jo, Kim *et al*. 2007). A reduction in size provides an exceptional surface area-to-volume ratio and changes in the surface energy, surface chemistry, and surface morphology of the particle, altering its basic properties and reactivity (Sobolev and Ferrada-Gutiérrez 2005, Sanchez and Sobolev 2010, Plassard, Lesniewska *et al*. 2004, Scrivener 2009, Bhushan 2004, Zhou, Liu *et al*. 2016, Penumadu, Dutta *et al*. 2009).

Nanosilica (silicon dioxide nanoparticles, nano- SiO$_2$), for example, has been shown to improve

---

∗Corresponding author, Professor, E-mail: r.kolahchi@gmail.com

workability and strength in high-performance and self-compacting concrete (Sanchez and Sobolev 2010). Most research on nanotechnology role in concrete industry has focused to date on the investigation of structure and mechanical properties of concrete at the nanoscale (Mart and Mijangos 2009, Dalton, Collins *et al*. 2004, Trtik and Bartos 2001). Recent advances in instrumentations have made it possible to characterize the structure of concrete at the nanoscale and to measure the local mechanical properties of its micro- and nanoscopic phases (Trtik and Bartos 2001). Significant progress in understanding nano-scale processes in cementations materials has been achieved thanks to the use of nano-scale characterization techniques (Trtik and Bartos 2001, Beaudoin 1999). These advanced techniques include nuclear magnetic resonance, atomic force microscopy, micro-and nano-indentation, neutron scattering, ultrasonic force microscopy, and focus-ion beam (FIB) nanotomography. For example, the use of atomic force microscopy (AFM) has revealed that, contrary to general thought, nanoscale C-S-H has in fact a highly ordered structure. A better understanding of the structure of concrete at the nano-level will allow for a better control of concrete performance and even the tailoring of desired properties and is expected therefore to affect the method of production and use of concrete.

Another application of nanotechnology in concrete has come from the "bottom-up" possibilities of nano-chemistry with the development of new products such as novel superplasticizers and new coating materials (Babazadeh, Burgueño *et al*. 2016, Corradi, Khurana *et al*. 2004). The development of coating materials with new self-cleaning properties, discoloration resistance, anti-graffiti protection, and high scratch-and-wear resistance is promising direction. In addition to these, self-cleaning materials based on photocatalyst technology were developed (Babazadeh, Burgueño *et al*. 2016). Titanium dioxide (TiO2) is used as a photocatalyst for the decomposition of organic compounds. TiO2 is active under exposure to UV light, exhibiting self-cleaning and disinfecting properties. Another aspect of self-cleaning is provided by the hydrophilicity of the surface, which helps to prevent dust and dirt from attaching to it. In the past, major developments in concrete technology have been achieved through the use of super-fine particles such as fly ash and silica fume. Recent advances in nano-chemistry and the development of new methods for synthesis of nanoparticles are now expected to offer a new range of possibilities for improvement of concrete performance (Collepardi, Ogoumah-Olagot *et al*. 2002, Flores, Sobolev *et al*. 2010). Incorporation of nanoparticles into conventional construction materials can provide the materials with advanced or smart properties that are of specific interest for high-rise, long-span, or intelligent infrastructure systems (Flores, Sobolev *et al*. 2010). The nonlinear buckling of straight concrete columns armed with single-walled carbon nanotubes (SWCNTs) resting on foundation was investigated by Jafarian Arani and kolahchi (2016).

To the best of authors' knowledge, no theoretical report has been found in the literature on buckling analysis of concrete columns reinforced with nanoparicles. Motivated by these considerations, in order to improve optimum design of concrete structures, we aim to present a mathematical model for simulation of embedded concrete columns reinforced with SiO_2 nanoparicles. The agglomeration effects are considered based on Mori-Tanaka approach. Herein, the structure is modelled with Euler-Bernoulli and Timoshenko beam models. The governing equations are obtained based on energy method and Hamilton's principal incorporating different boundary conditions. Using DQM, the buckling load of structure is calculated and the effects of different parameters such as volume percent of nanoparticles, geometrical parameters, elastic foundation and boundary conditions on the buckling load of concrete columns are shown.

2. Mori-Tanaka model and agglomeration effects

In this section, the effective modulus of the concrete column reinforced by SiO_2 nanoparticlesis developed. Different methods are available to obtain the average properties of a composite (Mori and Tanaka 1973). Due to its simplicity and accuracy even at high volume fractions of the inclusions, the Mori-Tanaka method (Mori and Tanaka 1973) is employed in this section. The matrix is assumed to be isotropic and elastic, with the Young's modulus E_m and the Poisson's ratio υ_m. The constitutive relations for a layer of the composite with the principal axes parallel to the r,θ and z directions are (Mori and Tanaka 1973)

$$\begin{Bmatrix} \sigma_{11} \\ \sigma_{22} \\ \sigma_{33} \\ \sigma_{23} \\ \sigma_{13} \\ \sigma_{12} \end{Bmatrix} = \begin{bmatrix} k+m & l & k-m & 0 & 0 & 0 \\ l & n & l & 0 & 0 & 0 \\ k-m & l & k+m & 0 & 0 & 0 \\ 0 & 0 & 0 & p & 0 & 0 \\ 0 & 0 & 0 & 0 & m & 0 \\ 0 & 0 & 0 & 0 & 0 & p \end{bmatrix} \begin{Bmatrix} \varepsilon_{11} \\ \varepsilon_{22} \\ \varepsilon_{33} \\ \gamma_{23} \\ \gamma_{13} \\ \gamma_{12} \end{Bmatrix}$$
(1)

where $\sigma_{ij}, \varepsilon_{ij}, \gamma_{ij}, k, m, n, l, p$ are the stress components, the strain components and the stiffness coefficients respectively. According to the Mori-Tanaka method the stiffness coefficients are given by (Mori and Tanaka 1973)

$$k = \frac{E_m\{E_m c_m + 2k_r(1+v_m)[1+c_r(1-2v_m)]\}}{2(1+v_m)[E_m(1+c_r-2v_m)+2c_m k_r(1-v_m-2v_m^2)]}$$

$$l = \frac{E_m\{c_m v_m[E_m+2k_r(1+v_m)]+2c_r l_r(1-v_m^2)]\}}{(1+v_m)[E_m(1+c_r-2v_m)+2c_m k_r(1-v_m-2v_m^2)]}$$

$$n = \frac{E_m^2 c_m(1+c_r-c_m v_m)+2c_m c_r(k_r n_r - l_r^2)(1+v_m)^2(1-2v_m)}{(1+v_m)[E_m(1+c_r-2v_m)+2c_m k_r(1-v_m-2v_m^2)]}$$
$$+ \frac{E_m[2c_m^2 k_r(1-v_m)+c_r n_r(1+c_r-2v_m)-4c_m l_r v_m]}{E_m(1+c_r-2v_m)+2c_m k_r(1-v_m-2v_m^2)}$$

$$p = \frac{E_m[E_m c_m + 2p_r(1+v_m)(1+c_r)]}{2(1+v_m)[E_m(1+c_r)+2c_m p_r(1+v_m)]}$$

$$m = \frac{E_m[E_m c_m + 2m_r(1+v_m)(3+c_r-4v_m)]}{2(1+v_m)\{E_m[c_m+4c_r(1-v_m)]+2c_m m_r(3-v_m-4v_m^2)\}}$$
(2)

where the subscripts m and r stand for matrix and reinforcement respectively. c_m and c_r are the volume fractions of the matrix and the nanoparticles respectively and k_r, l_r, n_r, p_r, m_r are the Hills elastic modulus for the nanoparticles (Mori and Tanaka 1973). The experimental results show that the assumption of uniform dispersion for nanoparticles in the matrix is not correct and the most

of nanoparticles are bent and centralized in one area of the matrix. These regions with concentrated nanoparticles are assumed to have spherical shapes, and are considered as "inclusions" with different elastic properties from the surrounding material. The total volume V_r of nanoparticles can be divided into the following two parts (Shi and Feng 2004)

$$V_r = V_r^{inclusion} + V_r^m \tag{3}$$

where $V_r^{inclusion}$ and V_r^m are the volumes of nanoparticles dispersed in the spherical inclusions and in the matrix, respectively. Introduce two parameters ξ and ζ describe the agglomeration of nanoparticles

$$\xi = \frac{V_{inclusion}}{V}, \tag{4}$$

$$\zeta = \frac{V_r^{inclusion}}{V_r}. \tag{5}$$

However, the average volume fraction c_r of nanoparticles in the composite is

$$C_r = \frac{V_r}{V}. \tag{6}$$

Assume that all the orientations of the nanoparticles are completely random. Hence, the effective bulk modulus (K) and effective shear modulus (G) may be written as

$$K = K_{out} \left[1 + \frac{\xi\left(\frac{K_{in}}{K_{out}} - 1\right)}{1 + \alpha(1-\xi)\left(\frac{K_{in}}{K_{out}} - 1\right)} \right], \tag{7}$$

$$G = G_{out} \left[1 + \frac{\xi\left(\frac{G_{in}}{G_{out}} - 1\right)}{1 + \beta(1-\xi)\left(\frac{G_{in}}{G_{out}} - 1\right)} \right], \tag{8}$$

where

$$K_{in} = K_m + \frac{(\delta_r - 3K_m\chi_r)C_r\zeta}{3(\xi - C_r\zeta + C_r\zeta\chi_r)}, \tag{9}$$

$$K_{out} = K_m + \frac{C_r(\delta_r - 3K_m\chi_r)(1-\zeta)}{3[1-\xi - C_r(1-\zeta) + C_r\chi_r(1-\zeta)]}, \tag{10}$$

$$G_{in} = G_m + \frac{\left(\eta_r - 3G_m\beta_r\right)C_r\zeta}{2\left(\xi - C_r\zeta + C_r\zeta\beta_r\right)},$$

(11)

$$G_{out} = G_m + \frac{C_r\left(\eta_r - 3G_m\beta_r\right)\left(1-\zeta\right)}{2\left[1-\xi - C_r\left(1-\zeta\right) + C_r\beta_r\left(1-\zeta\right)\right]},$$

(12)

where $\chi_r, \beta_r, \delta_r, \eta_r$ may be calculated as

$$\chi_r = \frac{3\left(K_m + G_m\right) + k_r - l_r}{3\left(k_r + G_m\right)},$$

(13)

$$\beta_r = \frac{1}{5}\left\{\frac{4G_m + 2k_r + l_r}{3\left(k_r + G_m\right)} + \frac{4G_m}{\left(p_r + G_m\right)} + \frac{2\left[G_m\left(3K_m + G_m\right) + G_m\left(3K_m + 7G_m\right)\right]}{G_m\left(3K_m + G_m\right) + m_r\left(3K_m + 7G_m\right)}\right\},$$

(14)

$$\delta_r = \frac{1}{3}\left[n_r + 2l_r + \frac{\left(2k_r - l_r\right)\left(3K_m + 2G_m - l_r\right)}{k_r + G_m}\right],$$

(15)

$$\eta_r = \frac{1}{5}\left[\frac{2}{3}\left(n_r - l_r\right) + \frac{4G_m p_r}{\left(p_r + G_m\right)} + \frac{8G_m m_r\left(3K_m + 4G_m\right)}{3K_m\left(m_r + G_m\right) + G_m\left(7m_r + G_m\right)} + \frac{2\left(k_r - l_r\right)\left(2G_m + l_r\right)}{3\left(k_r + G_m\right)}\right].$$

(16)

where, K_m and G_m are the bulk and shear moduli of the matrix which can be written as

$$K_m = \frac{E_m}{3\left(1 - 2\upsilon_m\right)},$$

(17)

$$G_m = \frac{E_m}{2\left(1 + \upsilon_m\right)}.$$

(18)

Furthermore, β, α can be obtained from

$$\alpha = \frac{\left(1 + \upsilon_{out}\right)}{3\left(1 - \upsilon_{out}\right)},$$

(19)

$$\beta = \frac{2\left(4 - 5\upsilon_{out}\right)}{15\left(1 - \upsilon_{out}\right)},$$

(20)

$$\upsilon_{out} = \frac{3K_{out} - 2G_{out}}{6K_{out} + 2G_{out}}.$$

(21)

Finally, the elastic modulus (E) and poison's ratio (υ) can be calculated as

$$E = \frac{9KG}{3K+G} \quad , \tag{22}$$

$$\upsilon = \frac{3K-2G}{6K+2G}. \tag{23}$$

3. Governing equations

Fig. 1 shows a concrete column reinforced with SiO$_2$ nanoparticles considering agglomeration effects. The surrounding foundation is described by the Winkler foundation model with spring constant K_w and Pasternak foundation model with shear constant G_p.

The concrete column is modeled with Euler-Bernoulli and Timoshenko beam models.

3.1 Euler-Bernoulli beam

The displacements of an arbitrary point in the Euler-Bernoulli beam are (Brush and Almorth 1975)

$$u_1(x,z) = U(x) - z\frac{\partial W(x)}{\partial x},$$
$$u_2(x,z) = 0,$$
$$u_3(x,z) = W(x), \tag{24}$$

where $U(x)$ and $W(x)$ are displacement components in the mid-plane. The von Karman type nonlinear strain–displacement relations are given by

$$\varepsilon_x = \left(\frac{\partial U}{\partial x}\right) + \frac{1}{2}\left(\frac{\partial W}{\partial x}\right)^2 - z\left(\frac{\partial^2 W}{\partial x^2}\right). \tag{25}$$
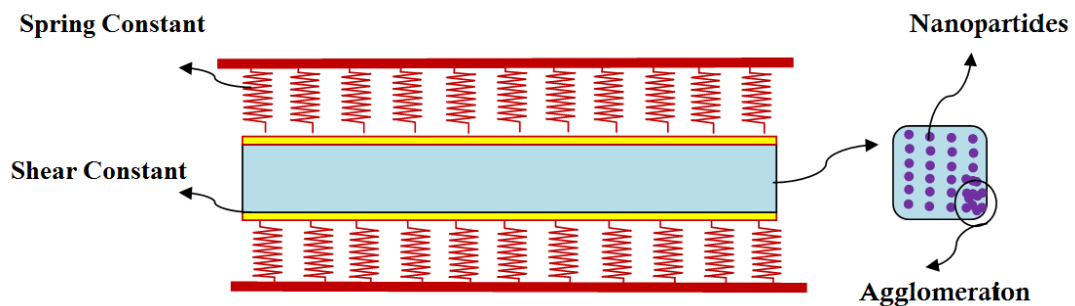

Fig. 1 Geometry of the concrete column reinforced with SiO$_2$ nanoparticles considering agglomeration effects

The stress-strain relations can be written as

$$\sigma_{xx} = C_{11}\varepsilon_x,$$

(26)

where C_{11} is elastic constant which can be calculated by Mori-Tanaka model. The strain energy of the structure can be expressed as

$$U = \frac{1}{2}\int_0^L \int_A (\sigma_{xx}\varepsilon_{xx})\ dAdx.$$

(27)

Submitting Eqs. (24) and (25) into (27) gives

$$U = \frac{1}{2}\int_0^L \left\{ N_x \frac{\partial U}{\partial x} + \frac{1}{2} N_x \left(\frac{\partial W}{\partial x} \right)^2 - M_x \frac{\partial^2 W}{\partial x^2} \right\} dx,$$

(28)

where the resultant force (N_x) and bending moment M_x, are defined in Appendix A. The external work due to the foundation can be written as (Ghorbanpour Arani, Kolahchi *et al.* 2015)

$$\Omega = \int_0^L \left(\underbrace{- K_w W + G_p \nabla^2 W}_{q} \right) Wdx.$$

(29)

The governing equations of structure can be derived from the Hamilton's principle as

$$\delta U : \frac{\partial N_x}{\partial x} = 0,$$

(30)

$$\delta W : \frac{\partial^2 M_x}{\partial x^2} - \frac{\partial}{\partial x}\left(N_x^M \frac{\partial W}{\partial x} \right) + q = 0,$$

(31)

where N_x^M is the axial load applied to the concrete column. Introducing the following dimensionless quantities

$$\xi = \frac{x}{L}, \quad (\overline{W}, \overline{U}) = \frac{(W, U)}{h}, \quad \eta = \frac{h}{L}, \psi = \overline{\psi}, \quad \overline{K}_w = \frac{K_w hL}{C_{11}A},$$

$$\overline{G}_p = \frac{G_p}{C_{11}A}, \overline{N}_x^M = \frac{N_x^M}{C_{11}A}, \overline{I} = \frac{I}{AL^2}, C_5 = \frac{C_{55}}{C_{11}}.$$

(32)

and substituting Eqs. (A4)-(A6) into the governing equations yields

$$\frac{\partial^2 \overline{U}}{\partial \xi^2} + \eta \frac{\partial^2 \overline{W}}{\partial \xi^2} \frac{\partial \overline{W}}{\partial \xi} = 0,$$

(33)

$$-\overline{I} \frac{\partial^4 \overline{W}}{\partial \xi^4} - \overline{N}_x^M \eta \frac{\partial^2 \overline{W}}{\partial \xi^2} - \overline{K}_w \overline{W} + \overline{G}_p \eta \left(\frac{\partial^2 \overline{W}}{\partial \xi^2} \right) = 0.$$

(34)

3.2 Timoshenko beam

The displacements of an arbitrary point in the Timoshenko beam are (Brush and Almorth 1975)

$$u_1(x,z) = U(x) + z\psi(x),$$
$$u_2(x,z) = 0,$$
$$u_3(x,z) = W(x),$$
(35)

where ψ is the rotation of beam cross-section

$$\varepsilon_{xx} = \frac{\partial U}{\partial x} + z\frac{\partial \psi}{\partial x} + \frac{1}{2}\left(\frac{\partial W}{\partial x}\right)^2,$$
(36)

$$\gamma_{xz} = \frac{\partial W}{\partial x} + \psi.$$
(37)

The stress-strain relations can be written as

$$\sigma_{xx} = C_{11}\varepsilon_x,$$
(38)

$$\sigma_{xz} = C_{55}\left[\frac{\partial W}{\partial x} + \psi\right],$$
(39)

where C_{11} and C_{55} are elastic constants which can be calculated by Mori-Tanaka model. The strain energy of the structure can be expressed as

$$U = \frac{1}{2}\int_0^L \int_A (\sigma_{xx}\varepsilon_{xx} + 2\sigma_{xz}\varepsilon_{xz})\, dAdx.$$
(40)

Submitting Eqs. (35) to (37) into (40) yields

$$U = \frac{1}{2}\int_0^L \left\{ N_x\frac{\partial U}{\partial x} + M_x\frac{\partial \psi}{\partial x} + \frac{1}{2}N_x\left(\frac{\partial W}{\partial x}\right)^2 + Q_x\frac{\partial W}{\partial x} + Q_x\psi \right\}dx.$$
(41)

The external work due to the foundation is the same as Eq. (29). The governing equations of structure can be derived from the Hamilton's principle as

$$\frac{\partial N_x}{\partial x} = 0,$$
(42)

$$\frac{\partial Q_x}{\partial x} - \frac{\partial}{\partial x}\left(N_x^M \frac{\partial W}{\partial x}\right) + q = 0,$$
(43)

$$\frac{\partial M_x}{\partial x} - Q_x = 0.$$
(44)

Based on dimensionless parameters in Eq. (32) and substituting Eqs. (A4)-(A6) into the governing equations yields

$$\frac{\partial^2 \overline{U}}{\partial \xi^2} + \eta \frac{\partial^2 \overline{W}}{\partial \xi^2} \frac{\partial \overline{W}}{\partial \xi} = 0,$$

(45)

$$C_5 \left[\eta \frac{\partial^2 \overline{W}}{\partial \xi^2} + \frac{\partial \overline{\psi}}{\partial \xi} \right] - \overline{N}_x^M \eta \frac{\partial^2 \overline{W}}{\partial \xi^2} - \overline{K}_w \overline{W} + \overline{G}_p \frac{\partial^2 \overline{W}}{\partial \xi^2} = 0,$$

(46)

$$\overline{I} \frac{\partial^2 \overline{\psi}}{\partial \xi^2} + K_s C_5 \left[\eta \frac{\partial \overline{W}}{\partial \xi} + \overline{\psi} \right] = 0.$$

(47)

4. DQM

The main idea of the DQM is that the derivative of a function at a sample point can be approximated as a weighted linear summation of the function value at all of the sample points in the domain. The functions f and their k^{th} derivatives with respect to x can be approximated as (Kolahchi, Rabani Bidgoli *et al*. 2015, Kolahchi, Safari *et al*. 2016a)

$$\frac{d^n f(x_i)}{dx^n} = \sum_{j=1}^{N} C_{ij}^{(n)} f(x_j) \qquad n = 1,...,N-1,$$

(48)

where N is the total number of nodes distributed along the x-axis and C_{ij} is the weighting coefficients, the recursive formula for which can be found in (Kolahchi and Moniribidgoli 2016b). Using DQM, the governing equations can be expressed in matrix form as

$$\left(\left[\underbrace{K_L + K_{NL}}_{K} \right] + P[K_g] \right) \begin{Bmatrix} \{d_b\} \\ \{d_d\} \end{Bmatrix} = 0,$$

(49)

where K_L is the linear stiffness matrix; K_{NL} is the nonlinear stiffness matrix and K_g is geometric stiffness matrix. Also, d_b and d_d represent boundary and domain points. Finally, based on an iterative method and eigenvalue problem, the buckling load of structure may be obtained.

5. Numerical results

The governing equations for buckling of structure are established for Euler–Bernoulli beam model and Timoshenko beam model in the last section. The material constants used in the calculation are: concrete column with elastic modules of $E_m = 20 \ GPa$ and SiO$_2$ nanoparticles with elastic modules of $E_r = 75 \ GPa$. Based on DQM, the buckling load of structure is calculated

and the effects of SiO_2 nanoparticles volume percent, geometrical parameters, elastic foundation and boundary conditions are showed.

At the first, the convergence and accuracy of DQM are studied for both Euler–Bernoulli and Timoshenko beam models. The effect of the grid point number in DQM on the buckling load of the concrete column is demonstrated in Figs. 2 and 3 for Euler-Bernoulli and Timoshenko beam models, respectively. As can be seen, fast rate of convergence of the method are quite evident and it is found that 15 DQM grid points can yield accurate results. In addition, with increasing thickness to length ratio (h/L) of column, the buckling load increases due to increase in stiffness of system.

In order to show the effect of SiO_2 nanoparticles volume percent in the concrete, Figs. 4 and 5 are plotted for Euler-Bernoulli and Timoshenko beam models, respectively. It can be found that with increasing the volume percent of SiO_2 nanoparticles, the nonlinear buckling load increases. It is due to the fact that with increasing volume percent of SiO_2 nanoparticles, the stiffness of structure increases. Hence, the SiO_2 nanoparticles volume fraction is effective controlling parameters for buckling of the concrete column. In addition, the buckling load predicted by Euler-Bernoulli model is higher than Timoshenko one. It is because that the flexibility of Timoshenko model is higher than Euler-Bernoulli model. Hence, the results predicted by Timoshenko beam model is more real with respect to Euler-Bernoulli one.
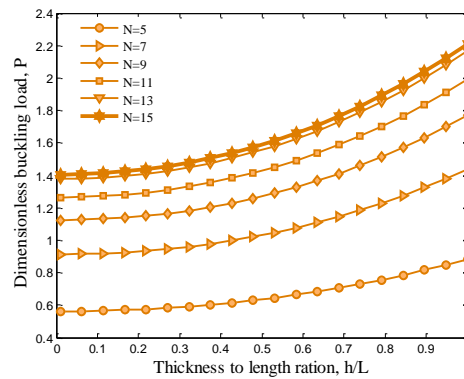
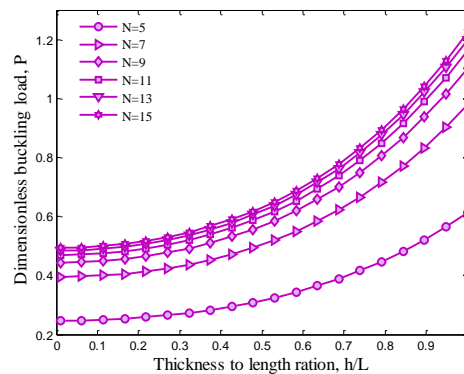

Fig. 2 Accuracy of DQM for Euler- Bernoulli beam model

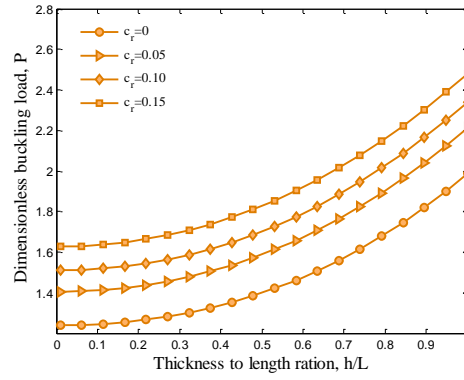Fig. 3 Accuracy of DQM for Timoshenko beam model

Fig. 4 The effect of SiO$_2$ nanoparticle volume percent on buckling load for Euler-Bernoulli beam model
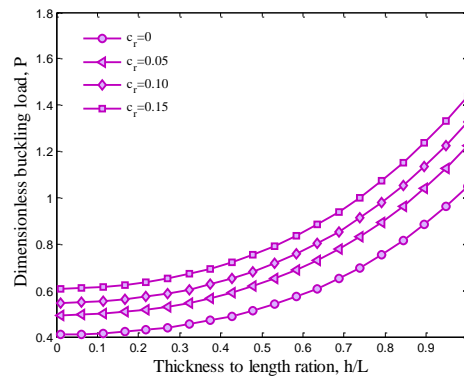

Fig. 5 The effect of SiO$_2$ nanoparticle volume percent on buckling load for Timoshenko beam model
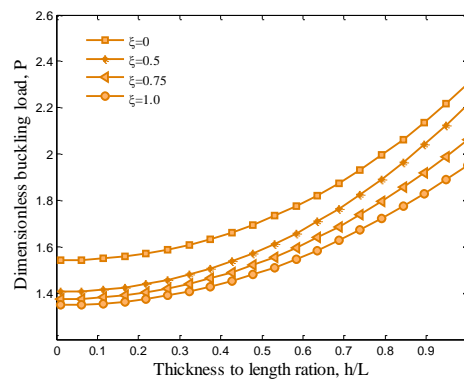

Fig. 6 Comparison of steel and SWCNT as reinforcer for Euler-Bernoulli beam model
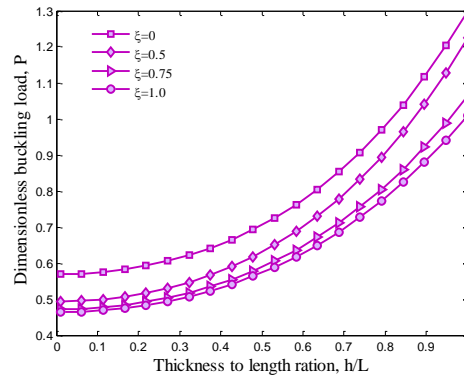
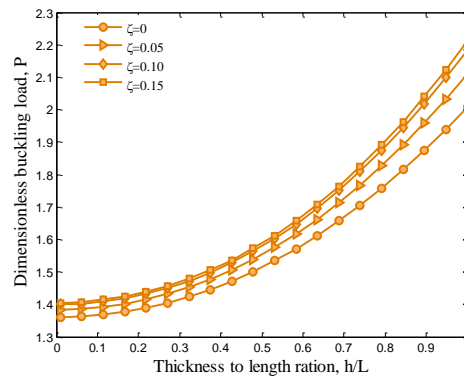Fig. 7 Comparison of steel and SWCNT as reinforcer for Timoshenko beam model

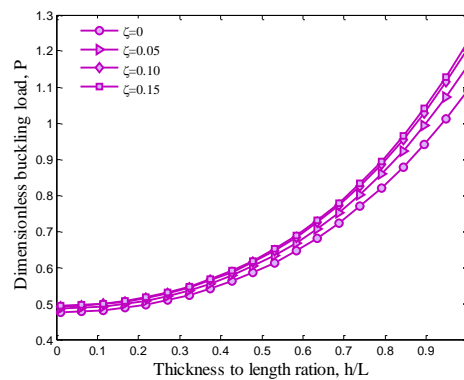Fig. 8 The volume percent of SiO$_2$ nanoparticles in inclusion effect for Euler-Bernoulli beam model

Fig. 9 The volume percent of SiO$_2$ nanoparticles in inclusion effect for Timoshenko beam model

The effects of agglomeration (ξ) respectively for Euler-Bernoulli and Timoshenko beam models, respectively on the buckling load along the thickness to length ratio are demonstrated in Figs. 6 and 7. It is worth noting that the buckling load decreases with increasing ξ. It is due to the fact that considering agglomeration effect leads to lower stiffness in structure. However, the agglomeration effect has a major effect on the buckling behaviour of structure. In addition, with increasing h/L ratio, the buckling load is increased for both models.

Figs. 8 and 9 illustrate the influence of volume percent of SiO$_2$ nanoparticles in inclusion (ζ) on the buckling load along the *h/L* ratio respectively for Euler-Bernoulli and Timoshenko beam models. It can be concluded that the buckling load is increased with increasing ζ. The above results are reasonable, since with increasing ζ the stiffness of structure increases.

6. Conclusions

Agglomeration effect on the buckling load of a concrete column reinforced with SiO$_2$ nanoparticles was the main contribution of this work. The column was simulated with Bernoulli and Timoshenko beam models mathematically. The characteristics of the equivalent composite were determined using Mori-Tanaka model. Applying DQM, the bulking load of structure is calculated and the effects of volume percent of SiO$_2$ nanoparticles, agglomeration and geometrical parameters are shown. Results indicate that with increasing the volume percent of SiO$_2$ nanoparticles, the nonlinear buckling load increases. In addition, the buckling load predicted by Euler-Bernoulli model was higher than Timoshenko one. It was also worth to mention that the buckling load of concrete column decreases with considering agglomeration effects. Obviously, with increasing volume percent of SiO$_2$ nanoparticles in inclusion, the buckling load was increased. Finally, it is hoped that the results presented in this paper would be helpful for mathematical modelling of concrete structures and using nanotechnology for production of them.

References

Babazadeh, A., Burgueño, R. and Silva, P.F. (2016), "Evaluation of the critical plastic region length in slender reinforced concrete bridge columns", *Eng. Struct.*, **125**, 280-293.

Beaudoin, J.J. (1999), "Why engineers need materials science", *Concrete Int.*, **21**, 86-89.

Bhushan, B. (2004), *Handbook of Nanotechnology*, Springer.

Brush, D.O. and Almroth, B.O. (1975), *Buckling of bars, plates and shells, McGraw-Hill*, New York.

Collepardi, M., Ogoumah-Olagot, J.J., Skarp, U. and Troli, R. (2002), "Influence of amorphous colloidal silica on the properties of self-compacting concretes", *Proceedings of the International Conference. Challenges in Concrete Construction - Innovations and Developments in Concrete Materials and Construction*, Dundee, UK.

Corradi, M., Khurana, R. and Magarotto, R. (2004), "Controlling performance in ready mixed concrete", *Concrete Int.*, **26**(8), 123-126.

Dalton, A.B., Collins, S., Razal, S.J., Munoz, E., Ebron, V.H., Kim, B.G., Coleman, J.N., Ferraris, J.P. and Baughman, R.H. (2004), "Continuous carbon nanotube composite fibers: properties, potential applications, and problems", *J. Mater. Chem.*, **14**, 1-13.

Flores, I., Sobolev, K., Torres, L.M., Valdez, P.L., Zarazua, E. and Cuellar, E.L. (2010), "Performance of cement systems with nano- SiO$_2$ particles produced using sol-gel method", *Proceedings of the TRB First*

International Conference in North America on Nanotechnology in Cement and Concrete, Irvine, California, USA, May 5-7.

Ghorbanpour Arani, A., Kolahchi, R. and Zarei, M. Sh. (2015), "Visco-surface-nonlocal piezoelasticity effects on nonlinear dynamic stability of graphene sheets integrated with ZnO sensors and actuators using refined zigzag theory", *Compos. Struct.*, **132**, 506-526.

Jafarian Arani, A. and Kolahchi, R. (2016), "Buckling analysis of embedded concrete columns armed with carbon nanotubes", *Comput. Concrete*, **17**(5), 567-578.

Jo, B.W., Kim, C.H. and Lim, J.H. (2007), "Investigations on the development of powder concrete with nano- SiO_2 particles", *J. Civil Eng. - KSCE*, **11**(1), 37-42.

Kolahchi, R. and and Moniribidgoli, A.M. (2016b), "Size-dependent sinusoidal beam model for dynamic instability of single-walled carbon nanotubes", *Appl. Math. Mech.*, **37**, 265-274.

Kolahchi, R., Rabani Bidgoli, M., Beygipoor, Gh. and Fakhar, M.H. (2015), "A nonlocal nonlinear analysis for buckling in embedded FG-SWCNT-reinforced microplates subjected to magnetic field", *J. Mech. Sci. Tech.*, **29**(9), 3669-3677.

Kolahchi, R., Safari, M. and Esmailpour, M. (2016a), "Dynamic stability analysis of temperature-dependent functionally graded CNT-reinforced visco-plates resting on orthotropic elastomeric medium", *Compos. Struct.*, **150**, 255-265.

Mart, J. and Mijangos, C. (2009), "Tailored polymer-based nanofibers and nanotubes by means of different infiltration methods into alumina nanopores", *Langmuir*, **25**(2), 1181-1187.

Mori, T. and Tanaka, K. (1973), "Average stress in matrix and average elastic energy of materials with misfitting inclusions", *Acta Metall. Mat.*, **21**(5), 571- 574.

Penumadu, D., Dutta, A.K., Luo, X. and Thomas, K.G. (2009), "Nano and neutron science applications for geomechanics", *J. Civil Eng.- KSCE*, **13**(4), 233-242.

Plassard, C., Lesniewska, E., Pochard, I. and Nonat, A. (2004), "Investigation of the surface structure and elastic properties of calcium silicate hydrates at the nanoscale", *Ultramicroscopy*, **100**(3-4), 331-338.

Sanchez, F. and Sobolev, K. (2010), "Nanotechnology in concrete - A review", *Construct. Build. Mater.*, **24**(11), 2060-2071.

Scrivener, K.L. (2009), *Nanotechnology and cementitious materials*, Proceed NICOM3 (3rd Int Symp Nanotech Const, Prague, Czech Republic.

Shi, D.L. and Feng, X.Q. (2004), "The effect of nanotube waviness and agglomeration on the elastic property of carbon nanotube-reinforced composties", *J. Eng. Mat. Tech.*, **126**(3), 250-270.

Sobolev, K. and Ferrada-Gutiérrez, M. (2005), "How nanotechnology can change the concrete world: Part 2", *The Americ. Ceramic Soc.*, **11**, 16-19.

Trtik, P. and Bartos, P.J.M. (2001), "Nanotechnology and concrete: what can we utilise from the upcoming technologies?", *Proceedings of the 2nd Annamaria Workshop: Cement Concrete : Trends & Challenges*.

Zhou, X., Liu, J., Wang, X. and Frank Chen, Y. (2016), "Behavior and design of slender circular tubed-reinforced-concrete columns subjected to eccentric compression", *Eng. Struct.*, **124**, 1 17-28.

CC

Appendix A

The resultant force (N_x, Q_x) and bending moment M_x, are defined as

$$N_x = \int_A \sigma_{xx} \, dA,$$

(A1)

$$M_x = \int_A \sigma_{xx} z \, dA,$$

(A2)

$$Q_x = K_s \int_A \sigma_{xz} \, dA,$$

(A3)

where K_s is shear correction factor. The work done by the foundation is denoted by (Ghorbanpour Arani, Kolahchi *et al*. 2015, Kolahchi, Rabani Bidgoli e*t al*. 2015). Substituting Eqs. (4) and (5) into Eqs. (8)-(10) yields

$$N_x = C_{11} A \frac{\partial U}{\partial x} + \frac{1}{2} C_{11} A \left(\frac{\partial W}{\partial x} \right)^2,$$

(A4)

$$M_x = C_{11} I \left[-\frac{\partial^2 W}{\partial x^2} + f(z) \left(\frac{\partial \psi}{\partial x} + \frac{\partial^2 W}{\partial x^2} \right) \right],$$

(A5)

$$Q_x = K_s C_{55} A \left[\frac{\partial W}{\partial x} + \psi \right].$$

(A6)